

Manuscript Number:

Title: New in-situ synthesized hydrogel composite based on alginate and brushite as a potential pH sensitive drug delivery system.

Article Type: Research Paper

Keywords: Alginate; brushite; Ibuprofen; Drug delivery system; in-situ hydrogel composite; pH sensitive

Corresponding Author: Mr. Seyed Mohammad Hossein Dabiri, Ph. D student

Corresponding Author's Institution: Univeristy of Genoa

First Author: Seyed Mohammad Hossein Dabiri, Ph. D student

Order of Authors: Seyed Mohammad Hossein Dabiri, Ph. D student; Alberto Lagazzo; Fabrizio Barberis; Amirreza Shayganpour; Elisabetta FINOCCHIO; Laura Pastorino

Abstract: A Series of in-situ alginate-brushite (Alg-Bru) hydrogel composites were fabricated in order to optimize release profile of ibuprofen (Ibu) and avoid burst releases associated with pure form of the hydrogels. The Bru crystals were synthesized and dispersed during the crosslinking process of Alg matrix. The beads with different formulations were subject to various characterization tests such as X-ray diffraction (XRD), fourier transform infrared spectroscopy (FTIR), scanning electron microscopy (SEM), dynamic mechanical analysis (DMA), and swelling. In addition, the entrapment efficiency (%EE) and drug release profile were obtained to investigate the impacts of initial concentration of Alg and content of Bru on these parameters. FTIR and XRD outcomes confirmed the successful fabricating of Alg-Bru composite and also loading of Ibu. Besides, the results showed that presence of Bru within Alg matrix restricted polymer chain movement and improved mechanical properties and decreased swelling ratio. Although the presence of Bru crystals did not improve %EE, they optimized the release profile in a more gradual manner.

Suggested Reviewers: Paola Petrini
Department of Bioengineering, Politecnico di Milano
paola.petrini@polimi.it
An expert professor in the field of drug delivery

Gleb Sukhorukov
School of Engineering and Materials Science, Queen Mary University of London
g.sukhorukov@qmul.ac.uk
He has been working in the area of drug delivery for a long period of time with expertise in the area of micro and nanoencapsulation

Yuri Lvov
Institute for Micromanufacturing, Louisiana Tech University
YLvov@latech.edu

He has been conducting so many researches on the micromanufacturing of polysaccharides for a wide range of medical applications

Dear editor

I would like to appreciate your kind review of the manuscript entitled “New in-situ synthesized hydrogel composite based on alginate and brushite as a potential pH sensitive drug delivery system.”

In the present study alginate-brushite composite hydrogels were in-situ synthesized at different concentration of alginate and content of brushite. The different samples were characterized using FT-IR, XRD, SEM, and dynamic mechanical analysis and swelling assay. The main objective of current study was improving mechanical properties and swelling behavior of calcium alginate by formation and dispersion of brushite crystals within the matrix. Furthermore, ibuprofen as a model drug was actively loaded on the above mentioned materials to evaluate the impact of brushite crystals on the in-vitro release behavior. Hence, a comparison between the samples prepared with different concentration of alginate, in the range of 1-2 %, and different initial phosphate precursor concentration, 0.1 M-0.4 M, was done to achieve this goal.

I look forward to your favorable considerations.

Yours sincerely

S. M. Hossein. Dabiri

PhD student at department of informatics, bioengineering, robotics, and system engineering- University of Genoa

Highlights

- Alginate-brushite hydrogel composites were in-situ synthesized and ibuprofen was actively loaded on them
- Formation of brushite within alginate caused the transformation of Na-ibuprofen to its acidic form
- The brushite within alginate matrix improved mechanical properties
- The brushite crystals restricted swelling behavior of alginate
- The increase in the initial concentration of phosphate precursor to 0.4 M resulted in less crosslinked beads
- The hydrogel composite beads release ibuprofen in a more controlled manner respect to calcium alginate one

New in-situ synthesized hydrogel composite based on alginate and brushite as a potential pH sensitive drug delivery system

Seyed Mohammad Hossein Dabiri^{a,*1}, Alberto Lagazzo^b, Fabrizio Barberis^b, Amirreza Shayganpour^{a,c},
Elisabetta Finocchio^b, Laura Pastorino^a

^a Department of informatics, bioengineering, robotics, and system engineering, University of Genova, Via All'Opera Pia, 13 - 16145 Genova, Italy

^b Department of Civil, Chemical and Environmental Engineering, University of Genova, p. J.F. Kennedy 1, 16129 Genova, Italy

^c Department of Nanophysics, Istituto Italiano di Tecnologia, via Morego 30, I-16163 Genova, Italy

Abstract

A Series of in-situ alginate-brushite (Alg-Bru) hydrogel composites were fabricated in order to optimize release profile of ibuprofen (Ibu) and avoid burst releases associated with pure form of the hydrogels. The Bru crystals were synthesized and dispersed during the crosslinking process of Alg matrix. The beads with different formulations were subject to various characterization tests such as X-ray diffraction (XRD), fourier transform infrared spectroscopy (FTIR), scanning electron microscopy (SEM), dynamic mechanical analysis (DMA), and swelling. In addition, the entrapment efficiency (%EE) and drug release profile were obtained to investigate the impacts of initial concentration of Alg and content of Bru on these parameters. FTIR and XRD outcomes confirmed the successful fabricating of Alg-Bru composite and also loading of Ibu. Besides, the results showed that presence of Bru within Alg matrix restricted polymer chain movement and improved mechanical properties and decreased swelling ratio. Although the presence of Bru crystals did not improve %EE, they optimized the release profile in a more gradual manner.

Key words:

*Corresponding author
Email: mohammadhossein.dabiri@gmail.com

Alginate, brushite, Ibuprofen, Drug delivery system, in-situ hydrogel composite, pH sensitive

1. Introduction

In the last years, drug delivery systems (DDS) have risen the attention as an optimized therapeutic method of drug administration. One of the main aim of these systems is to control the release profile of drugs in order to have a sustained therapeutic level and to minimize adverse side effects [1]. Among the materials, which have been proposed for the fabrication of DDS, hydrogels are of particular interest due to their biodegradability, biocompatibility, and also stimuli responsive characteristics [2]. Several hydrogels based on of polymers, such as alginate [3], chitosan [4], gelatin [5], polyvinyl alcohol (PVA) [6] poly (ethylene glycol) (PEG) [7] and so on, have been widely used as carriers for drugs, cells and proteins. However, such applications of pure hydrogels experience the phenomenon of burst release since hydrogels are highly water contended and possess weak mechanical properties [8].

Alginate (Alg) is a promising biopolymer which has numerous biomedical application ranging from wound healing to drug delivery and cell transplantation in tissue engineering [9, 10]. This anionic polysaccharide is typically extracted from brown seaweed and composed of α -L-guluronic acid (G) and the β -D-mannuronic acid (M) [11]. Alg gelation occurs as a result of exchanging sodium ions of G-blocks with multivalent cations like Ca^{2+} , Ba^{2+} , Sr^{2+} , Zn^{2+} to form electrostatic held junction [12]. Besides, Alg presents pH sensitive swelling behavior which makes it a potential candidate as drug carrier for oral administration, since it protects the entrapped drug in the gastric fluid and release it in intestine fluid [13]. Yet, it has been reported that Alg has a low encapsulation efficiency of water-soluble drug because of drug leakage during crosslinking procedure. In addition, the fast integration in intestine fluid as well as the highly porous structure of Alg are two other major limitations to the use of this polysaccharide. One

useful solution seems to be increasing the number of cross-links which will result in decreasing the swelling ratio [14-17].

Another solution which can be adopted is improving mechanical properties via incorporation of other phases inside the hydrogel matrix. Various papers focused on fabricating biopolymer-inorganic reinforcement hydrogel composites to improve mechanical properties by restricting polymeric chain movements [18-21]. Besides, further improvements seem to be achievable by changing type of reinforcement and also the content of polymer and inorganic compound. Indeed, this incorporation must not affect the structure of the Alg and also must not result in cytotoxic behavior [21].

Calcium phosphate materials, mainly hydroxyapatite, have been incorporated into Alg to prolong the release profile. Previously Zhang et al [22] showed that in-situ synthesized hydroxyapatite micro particle within Alg restricted the polymer chain movement and consequently decreased the swelling ratio. In addition, they demonstrated that incorporating of hydroxyapatite improved the entrapment efficiency and prevented burst release. Also, Ilie et al [23] studied the release of ascorbic acid, Vitamin C, from Alg-hydroxyapatite composite and demonstrated the significant impact of hydroxyapatite on gradual release of ascorbic acid. In another paper, hydroxyapatite nanoparticles were introduced into Alg-poly (vinyl pyrrolidone) blends and diclofenac sodium release was investigated starting from several compositions of these carriers [24]. The release profile indicated that presence of nanohydroxiapatite particles not only improved the loading efficiency, but also it remarkably decreased the amount of released drug.

Brushite, dicalcium phosphate dihydrate, (Bru) is a calcium phosphate material with Ca/P ratio of one. Biodegradability of Bru is the unique advantage of it over other calcium phosphate materials [25]. Previously, we investigated the in situ synthesis of Alg- Bru composite

hydrogel and optimized the fabrication method. Moreover, we evaluated the biocompatibility of these materials respect to osteoblastic cell and observed a significant improve in cell proliferation respect to calcium Alg [26, 27]. In the current study, we focused on the in-situ fabrication of Alg-Bru hydrogel composites as drug carriers and evaluated them in terms of mechanical properties and swelling behavior. Sodium salt of Ibu was used as a model drug to perform release experiments in order to deeply investigate the mechanical properties impact on the release behavior of these composite materials.

2. Materials and methods

2.1. Raw materials

All the chemical reagents: sodium Alg from brown algae with a viscosity of 15-20 cps at the concentration of 1%, calcium nitrate tetrahydrate [$\text{Ca}(\text{NO}_3)_2 \cdot 4\text{H}_2\text{O}$, 99%], diammonium hydrogen phosphate [$(\text{NH}_4)_2\text{HPO}_4$, 98%], hydrochloric acid (HCl), sodium hydroxide (NaOH), potassium dihydrogen phosphate (KH_2PO_4), phosphate buffered saline (PBS) tablets, and Ibu sodium salt were supplied by Sigma-Aldrich. All reagents were used without any purification. A Milli-Q system with the resistance of 18.2 M Ω cm was used to purify water which was consequently used for preparing solutions and washing steps.

2.2. Beads preparation

A series of Alg-Bru beads were prepared according to the following procedure. First, a predetermined amount of di-ammonium hydrogen phosphate was dissolved in 10 ml of purified water at room temperature and 600rpm. Then, accurately weighted amounts of sodium Alg were added slowly to the above solution under stirring rate of 600rpm. This solution was stirred for two hours to ensure that Alg completely dissolved. After that, the solution was dripped at room

temperature into the crosslinking solution (0.2 M of calcium nitrate) with gentle stirring (50 rpm) through a syringe equipped with a 0.8 mm needle. The initial pH of the solutions was maintained at 7.5 using HCl and NaOH (0.1M). White beads were formed immediately and maintained in the crosslinking solution to ensure that the Bru crystal growth and crosslinking process were properly accomplished. Thereupon, the samples were centrifuged at 1000rpm for 5 minutes and rinsed 4 times to remove excess Ca^{2+} and other impurities. Finally, the samples were kept for 24 h at room temperature and placed in the oven for 12 hours at 45°C.

In order to prepare Ibu loaded beads, predetermined amounts of Ibu were added to the aqueous solutions composed of di-ammonium hydrogen phosphate and sodium Alg. The solutions were stirred for 1h to ensure that Ibu completely dissolved in the media. The rest of procedure, including crosslinking and washing steps were done as described above. In addition, calcium Alg samples were prepared following the above procedure except that no $(\text{NH}_4)_2\text{HPO}_4$ was added to the Alg solution. The factors significantly impacting on the swelling behavior, drug loading, and drug release behavior, such as initial concentration of Alg, and primary concentration of phosphate precursor were summarized in table 1.

Table. 1 preparation conditions and their influence on swelling ratio and storage modulus

Item	Sample	Sodium alginate (wt %)	(NH ₄) ₂ HPO ₄ (M)	Ca(NO ₃) ₂ ·4H ₂ O (M)	Swelling ratio	Storage modulus at 10 Hz (kPa)	Storage modulus at 85 Hz (kPa)
1	Alg 1.5	1.5	---	0.2	12.72±1.00	21.47±4.17	30.5±3.17
2	Alg 1- P 0.1	1	0.1	0.2	7.00±0.63	24.63±2.57	35.2±3.54
3	Alg 1.5- P 0.1	1.5	0.1	0.2	10.29±0.37	40.37±2.01	58.83±3.42
4	Alg 2- P 0.1	2	0.1	0.2	11.38±0.44	56.43±6.14	78.86±6.53
5	Alg 2-P 0.2	2	0.2	0.2	9.13 ±1.59	85.96±5.31	119.47±6.35
6	Alg 2-P 0.4	2	0.4	0.2	8.65± 1.67	54.66±10.22	73.93±14.84
7	Alg 2	2	0.2	0.2	13.57±0.62	49.57±9.73	70±8.21

2.3. Characterization

A Nicolet 380 Fourier transform infrared spectrometer (Thermo Fisher scientific Inc, USA) was used to obtain FT-IR spectra by KBr technique and evaluate the formation of composite and interactions between Ibu and composite materials. The spectra were collected within the range of 400 to 4000 cm⁻¹. In order to identify the inorganic phase of beads as well as presence of the entrapped drug, beads were subject to X-ray diffraction (XRD) test. Therefore, A PANalytical Empyrean x-ray diffractometer with irradiation source of Cu-K α was used to collect the spectra over the Bragg angle, 2 θ , range of 5-60 at a scan rate of 2° per minute. The obtained spectra were compared with those of standard JCPDS numbers for Bru (9-0077) and Ibu (32-1723). A scanning electron microscopy (Hitachi S-2500) was used to investigate the dispersion of Bru crystals in Alg matrix and morphology of Bru crystals.

2.4. Dynamic mechanical analysis (DMA)

A typical test to gather information about mechanical properties of hydrogels is dynamic mechanical analysis (DMA). The mechanical properties of different hydrogel samples were obtained using a custom-made device, figure S1, developed at DICCA laboratory of University

of Genova. All the tests were performed in compression, in the range 5-100 Hz, with an initial pre-deformation of 20% of the sample diameter. The test consists in a sinusoidal vertical oscillation of the plate on which is lent the hydrogel sample obtained with a shaker (*Briuel & Kjaer, Mini-shaker, type 4810*), at which correspond a sinusoidal deformation of the sample due to the action of a cylindrical indenter. The corresponding sinusoidal oscillating force, dynamic oscillating stimulus, is measured with a force transducer (*PCB Piezotronic, Load cell, model 208 M116*) with the accuracy of 10^{-3} N, while the displacement is evaluated with an resolution of 0.01 μm through a laser vibrometer (*Polytec OFV 3000 vibrometer controller*), focused on the oscillating plate. Table. S1 summerized the set-up parameters of the device.

The dynamic complex modulus, E^* , defines as the stress to strain amplitude ratio of the materials placed in the vibration conditions.

$$\text{Equ.1 } E^* = \frac{\sigma}{\varepsilon}$$

The complex modulus can be split in two parts according to the Equ.1:

$$\text{Equ.2 } E^* = E' + iE''$$

Where

$$\text{Equ.3 } E' = E^* \cos \delta = \frac{\sigma}{\varepsilon} \cos \delta \text{ is the storage (or elastic) modulus}$$

$$\text{Equ.4 } E'' = E^* \sin \delta = \frac{\sigma}{\varepsilon} \sin \delta \text{ is the loss (or damping) modulus}$$

The Storage Modulus represents the elastic component of the material and it indicates the amount of energy stored during a loading cycle. The Loss Modulus, instead, represents the viscous component and it is proportional to the energy dissipated, such as heat, during the same loading cycle. Both E' and E'' are dynamic material-specific characteristics that depend on the

frequency as well as the measuring conditions. The behavior of a material is conventionally called solid-like when $E' > E''$ at a given frequency, namely when the loss factor, $\tan \delta < 1$, otherwise it is defined as liquid-like. The loss factor (Q^{-1}) is the ratio of loss modulus to storage modulus and it is a measure of the energy lost, expressed in terms of the recoverable energy. It represents the mechanical damping or internal friction in a viscoelastic system. The phase angle δ is the phase difference between the dynamic stress and the dynamic strain in a sample subjected to a sinusoidal oscillation. For a viscoelastic material δ falls into the following range:

$$0 < \delta < \pi/2$$

2.5. Swelling ratio

The swelling ratio of the micro beads was calculated gravimetrically by measuring their weight gain in phosphate buffer saline (PBS) at pH 7.4. Accurately weighted (W_0) and dried micro beads were immersed in PBS at 37° C. After predetermined time intervals (30, 60, 90, 120, 180, 240, 300, and 360 minutes?), the beads were filtered from the solution through a Millipore 0.22 μ filter equipped with a pump to remove extra liquid and weight immediately (W_t). The following equation will give us swelling ratio (SR) of micro beads at different time.

$$SR = \left(\frac{W_t - W_0}{W_0} \right)$$

2.6. Drug content

In order to estimate drug encapsulation efficiency, 10 mg of dried beads was placed and shaken in 10 ml of PBS for 24 h at 37° C, and then sonicated (FALC-HK2200, Italy) for 30 minutes in order to ensure a complete IBU release. After that, the solution was centrifuged and filtered using Minisart 5.00 μ filter. The actual amount of IBU was determined using a UV visible

spectrophotometer (Jasco V-570) at the wavelength of 264 nm and a calibration curve in PBS. Then, the entrapment efficacy (% EE) for Ibu was calculated according to the following equation:

$$\% \text{ EE} = \left(\frac{\text{Actual drug loading}}{\text{Theoretical drug loading}} \right) \times 100$$

2.7. In-vitro drug release experiment

In vitro drug release of Ibu from the different formulation of Alg-Bru samples was carried out at 37 °C using Heraeus incubator equipped with an IKALABORTECHNIK shaker at the rotation speed of 100 rpm in PBS. The first two hours of experiments were carried out in a PBS solution at pH 1.5 (prepared by dissolving 0.05M of KH_2PO_4 and adding HCl to adjust the pH) and followed by 8 hours in PBS solution at pH 7.4 to simulate the behavior of the carrier in the gastric fluid and intestine fluid, respectively. 10 mg of dried hydrogel samples were immersed in a 10 ml of release media. After predetermined time intervals, 5 ml of solution was withdrawn and replaced with equal amount of fresh media. These withdrawn samples were subject to UV visible spectrophotometer at 264 nm. The IBP release percentage was calculated according to following equation:

$$\text{IBP release percentage} = (R_t / R_0) \times 100$$

Where R_t is the released amount of IBP at time t and R_0 is initial amount of Ibu encapsulated in the beads.

3. Result and Discussion

Previously we investigated the mechanism of in-situ fabrication of these hydrogel composites [26]. Briefly, two simultaneous phenomena occurred as a result of in-situ synthesized method which was used to fabricate the hydrogel composites. First, the nucleation and growth of Bru

crystals inside the Alg matrix occurs, followed by crosslinking of the polymeric network and formation of the 3D structure of beads. IBU was loaded into the beads by dissolving it in the solution containing sodium Alg and $(\text{NH}_4)_2\text{HPO}_4$. This procedure started as soon as the polymeric solution was introduced to the crosslinking solution in a dropwise manner. The homogeneous dispersion of Ca^{2+} and PO_4^{3-} ions in both solution would yield to uniform dispersion of Bru crystals within the Alg matrix. As reported before [22] the concentration of $(\text{NH}_4)_2\text{HPO}_4$ and sodium Alg significantly impacts on the mechanical properties, swelling ratio, entrapment efficiency, and in-vitro release behavior. Therefore, we investigated the influence of the following factors on the mentioned characteristics. In addition, the initial drug content is another significant factor owing to its interaction with the carrier in the molecular scale. Hence, we studied the loading efficiency and its consequent in vitro release for three different concentration of drugs.

3.1.Characterization

3.1.1. FT-IR analysis

Fig. 1 shows the IR spectra of Alg -Bru hydrogel composite and Ibu loaded Alg-Bru hydrogel composite in comparison to spectra of pure reference materials, i.e. calcium Alg, Bru and, Ibu. In the spectrum of the Ibu-loaded composite several bands are detected, characterizing both the hydrogel matrix and the drug molecule. In the high frequency region, the two doublets are diagnostic peaks of Bru which corresponds to O-H stretching peaks of the two structural water molecules [28]. These peaks in our spectrum were detected at $3164, 3278 \text{ cm}^{-1}$ and $3496, 3546 \text{ cm}^{-1}$. Furthermore, the corresponding sharp peak to the H-O-H bending mode was observed at 1640 cm^{-1} [29]. The peaks at $1133, 1056$ and 985 cm^{-1} represent the specific peaks of PO_4 [28, 30]. Besides, the bands at 1226 and 869 cm^{-1} indicates stretching mode of P-OH and bending

mode of P-OH, respectively [29]. Moreover, P-O deformation mode of phosphate group were observed at 659, 574 and 526 cm^{-1} [28]. On the other side, the broad bands centered at 1640 and 1425 cm^{-1} , which represent the asymmetric and symmetric stretching mode of the carboxyl group in Alg spectrum [31] appear as very weak absorptions, partially masked by the Bru strong features. Also the complex peak in the range of 1000-1200 cm^{-1} due to C-O and C-C stretching modes of in the Alg chain [31] is overlapped with bands of the phosphate group.

As for the Ibu molecules loaded in the complex matrix, the band at 1720 cm^{-1} is assigned to C=O stretching vibration of the undissociated (acidic) COOH group, while weak and sharp bands at 1508, 1461, and 1384 cm^{-1} can be attributed to C-C vibrational modes in phenyl ring and vibration of C-H bond in the Ibu structure [4,32,33]. In the same figure, the spectrum of Ibue in form of Na-salt is reported for comparison, characterized by two strong bands at 1550 and 1412 cm^{-1} , which are assigned to the asymmetric and symmetric vibrational modes of the $-\text{COO}-$ group.

The subtraction spectrum [Alg-Bru-Ibu spectrum] – [Alg- Bru spectrum] reported in Fig. 2 evidenced two main effects arising from the drug entrapment: i) the two strong bands appearing in the spectrum of the pure Na-Ibu and due to asymmetric and symmetric stretching modes of the salt are not detected anymore, replaced by the sharp band at 1720 cm^{-1} ($\nu\text{C}=\text{O}$ of the $-\text{COOH}$ group);ii) other bands of the drug molecules, for instance bands due to alkyl chain and aromatic ring, are clearly detectable and only very slightly affected by the interaction with the composite. A likely explanation is that the pH decreasing during Bru formation in the matrix [34] leads to the formation of free COOH groups in the acidic form of Ibu. Inclusion of the drug in its acidic (neutral) form within the beads might be favored in comparison with the inclusion of the

corresponding anionic form, by reducing the electrostatic repulsion with negatively charged Alg chains.

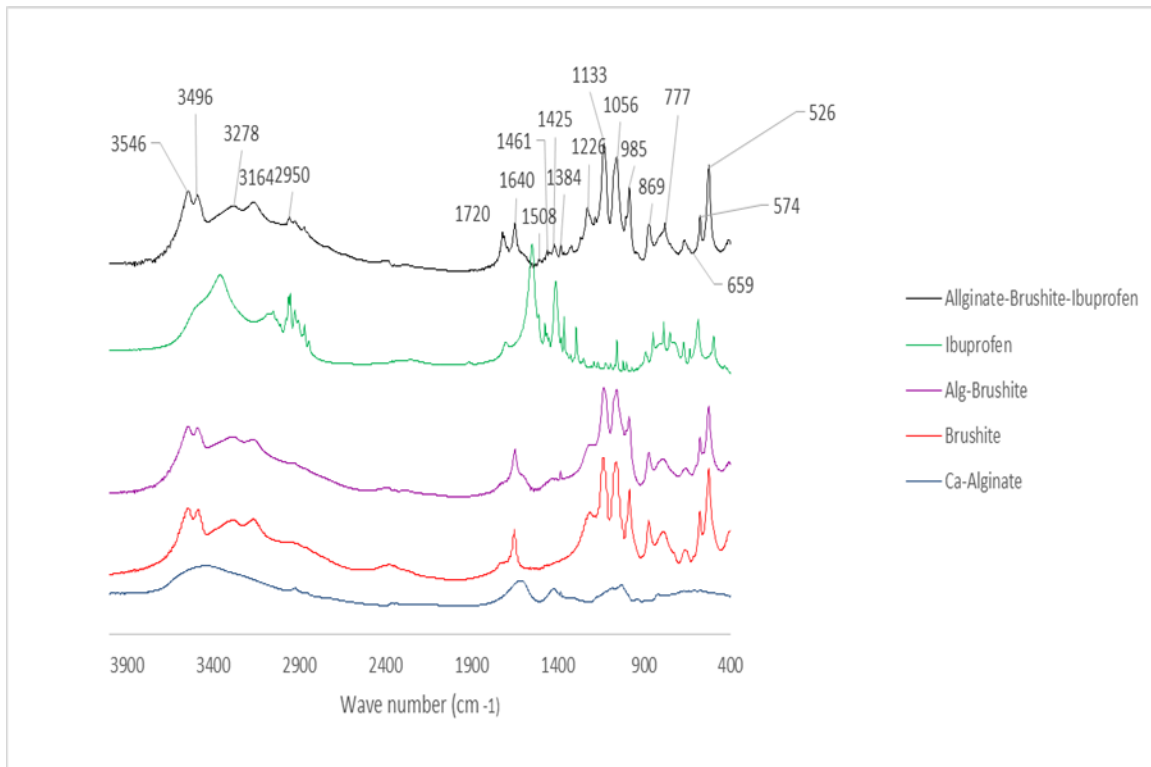


Fig. 1 FT-IR spectra of calcium alginate, brushite, alginate-brushite, ibuprofen, and ibuprofen loaded alginate-brushite

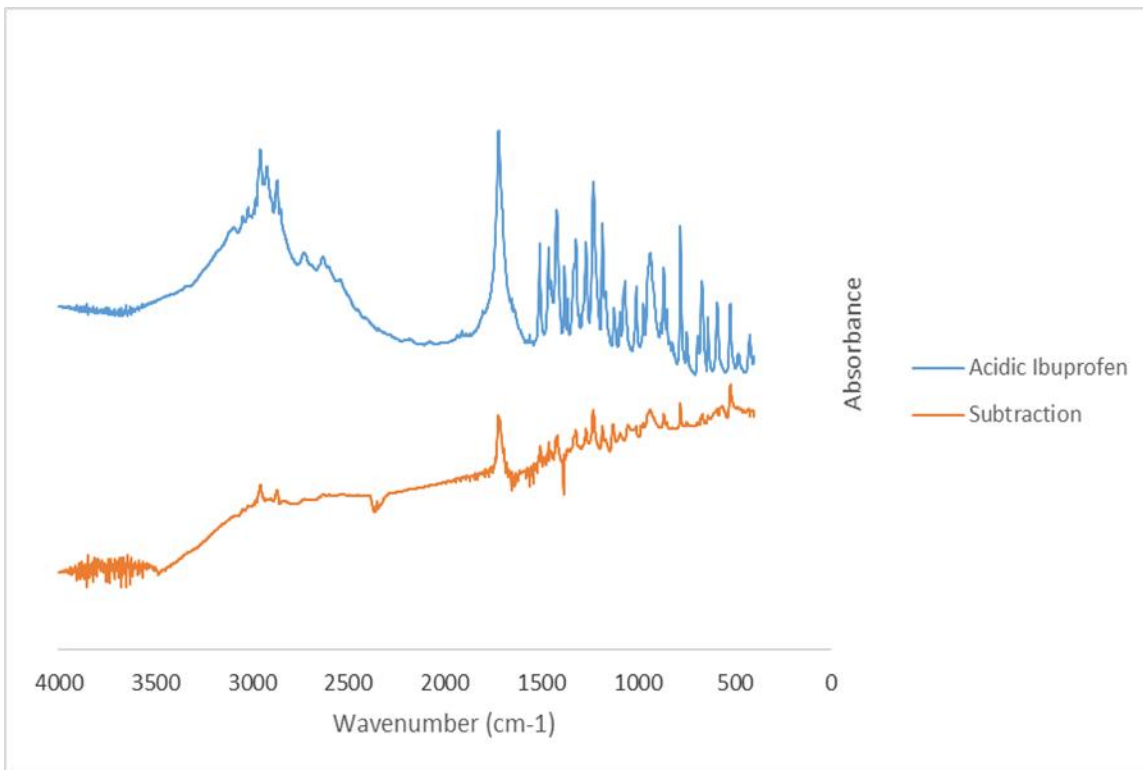


Fig. 2 FT-IR spectrum of acidic ibuprofen and subtraction spectrum [Alg-Bru-Ibu] – [Alg-Bru]

3.1.2 X-Ray diffraction

Fig. 3 shows the XRD patterns of Alg-Bru hydrogel composite, Ibu, and Ibu loaded Alg-Bru hydrogel composite. The standard Bru JCPDS card (9—0077) and the standard Ibu JCPDS card (32-1723) were used to analyze the resultant spectra. As we can see in Fig. 3, those peaks marked by red * are characteristic peaks of Ibu. In addition, those peaks with blue * are mutual peaks of Bru and Ibu. The rest of peaks relate to characteristic peaks of Bru component. Hence, the FT-IR results along with those of XRD confirmed that the drug successfully was entrapped by Alg-Bru beads.

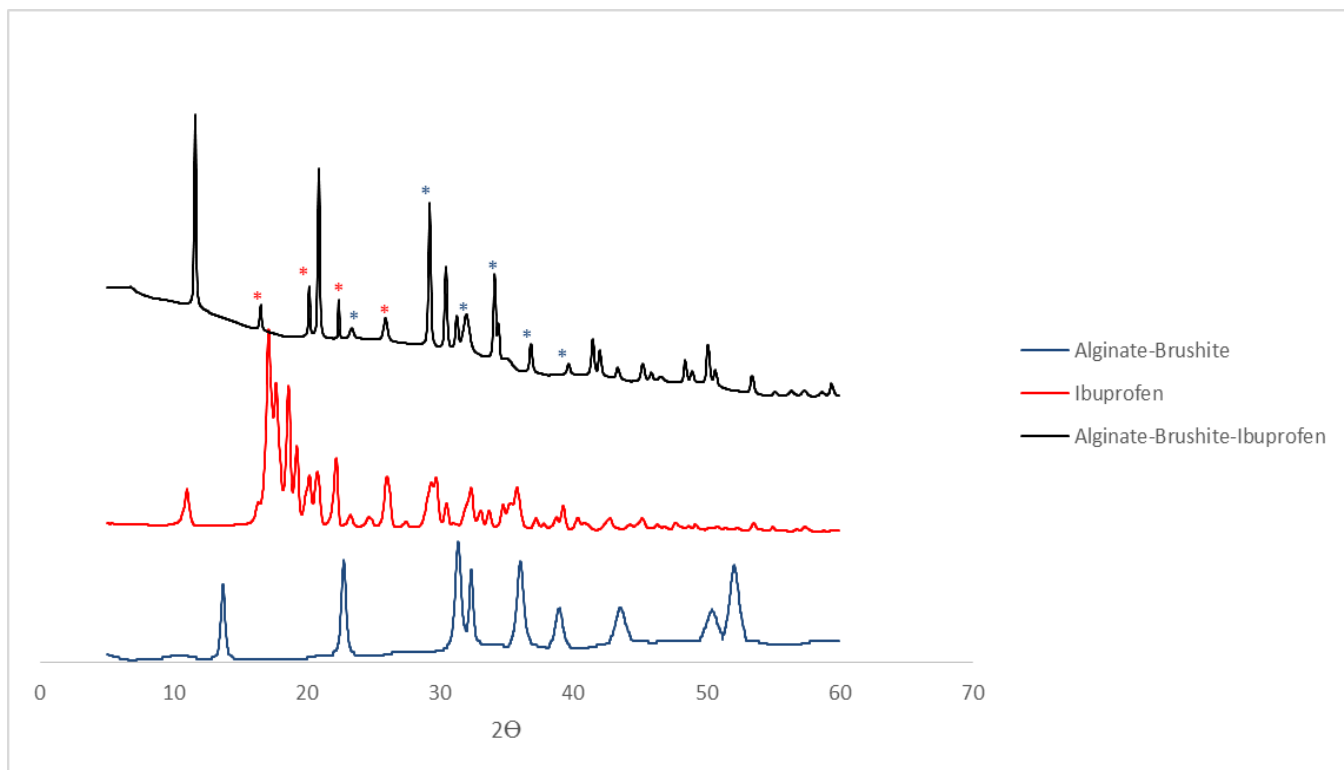
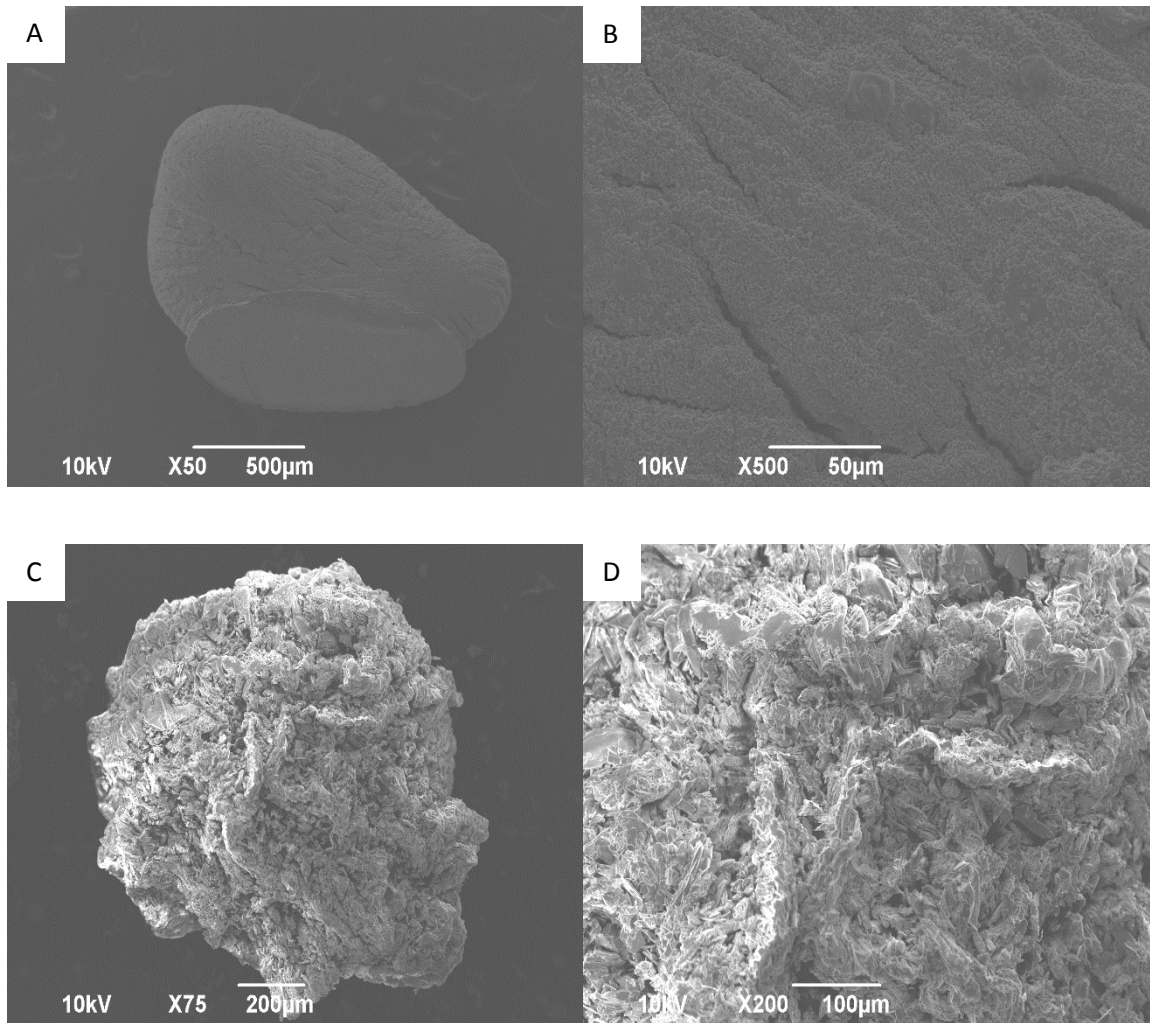


Fig. 3 XRD patterns of alginate-brushite, ibuprofen, and ibuprofen loaded alginate-brushite

3.1.3. Scanning electron microscopy (SEM)

The SEM micrograph of calcium Alg and Alg-Bru dried beads at different magnification are presented in Fig. 4A, 4B, 4C, 4D, 4E and 4F to investigate the impact of phosphorus group incorporation on the surface morphology of beads. In addition, Fig. 4G presents the EDS spectra of the beads to have an elemental analysis of the dried beads. It has been reported [22] that the dried beads of calcium Alg have a round, tight, and soft surface whilst, the Alg-Bru beads present an irregular shape and rough surface with considerable wrinkles. Angadi et al [35] claimed quick drying process as well as heterogeneous structures was the main reason for irregular shape of Alg composite dried beads. Higher magnification images demonstrated the accumulation of Bru plate-like crystals with various dimension in the Alg matrix. Furthermore, the elemental analysis of the dried beads from EDS showed the presence of Ca, P, Na, C, and O.

The calcium content relates to both calcium Alg and Bru, while the phosphorous content can be attributed only to the Bru. In addition, Na is also detected due to presence of small amount of residual sodium Alg.



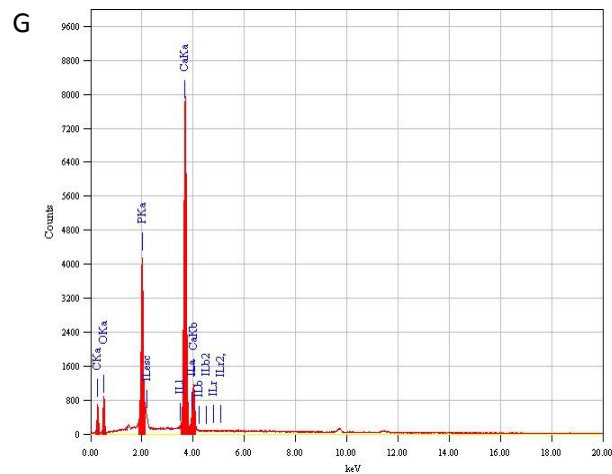
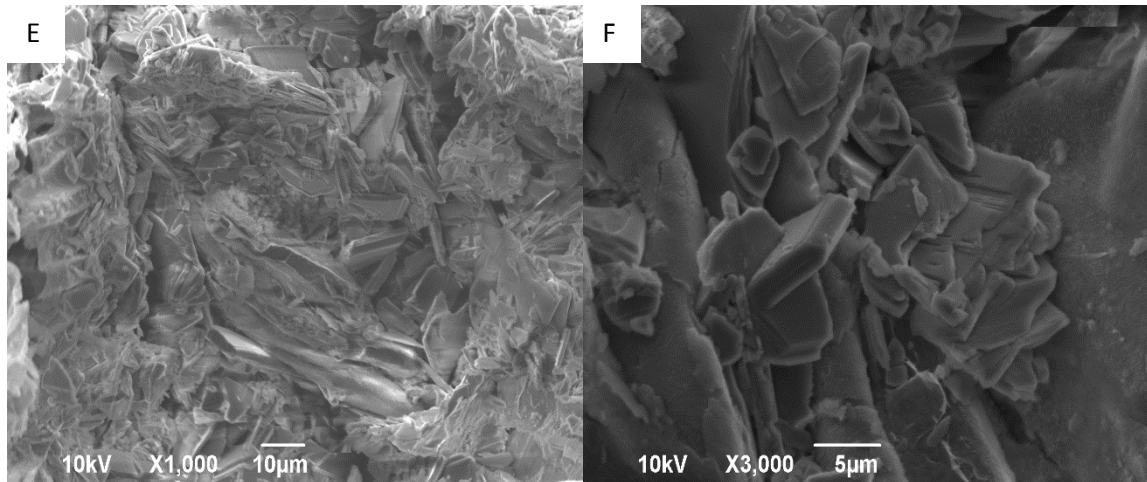


Fig. 4 the SEM micrograph of Alg 1.5 at A: 50x B: 500x and Alg 2-P 0.2 sample at C: 75x, D: 200x, E: 1000, F: 3000x, G: EDS spectra of Alg 2-P 0.2

3.1.4. Dynamic mechanical analysis (DMA)

Fig. 5A, 5B, and table. 1 present DMA results of different composite and reference samples versus frequency. As we can see, the loss factor (Q^{-1}) < 1 in all samples indicating that all the hydrogel samples presented a solid like behavior. Furthermore, as the concentration of Alg increased, the storage modulus showed an upward trend Fig. 6. Almost 35 kPa enhancement in the storage modulus of composite samples seemed to be considerable when the concentration of

Alg increased from 1% to 2%. This improvement can be attributed to the fact that an increase in the concentration of Alg led to a denser polymeric chain. In addition, higher crosslinking density, likely due to an increase in the electrostatic attraction between carboxylate groups of Alg and calcium ions can explain this improvement [36]. The comparison between the Alg 1.5 and Alg 1.5-P 0.4 samples, which were composed of equal Alg concentration, revealed more than 20 kPa improvement in the storage modulus. This relates to the fact that Bru component has higher mechanical properties than Alg and the polymeric chains movements are restricted by the crystalline component.

The impact of Bru content on the storage modulus at different frequency can be seen in the Fig. 5B and Fig. 6. It is clear that storage modulus at different frequency, i.e. 10 and 85 Hz, was significantly enhanced by increasing in the content of Bru. However, this improvement was followed by a remarkable decrease when higher content of Bru (Alg 2-P 0.4) was introduced into the sample. This can be explained by the fact that the higher amount of PO_4^{3-} in the Alg 2-P 0.4 sample is acting as a barrier in the crosslinking process. Therefore, the sample Alg 2-P 0.4 is less crosslinked than the other two as evidenced by storage modulus results, although the higher amount of Bru crystal reduces the mobility of the polymeric chains, conferring to the specimen a further increase of their solid-like status, reduction of the loss factor (Fig. 5B).

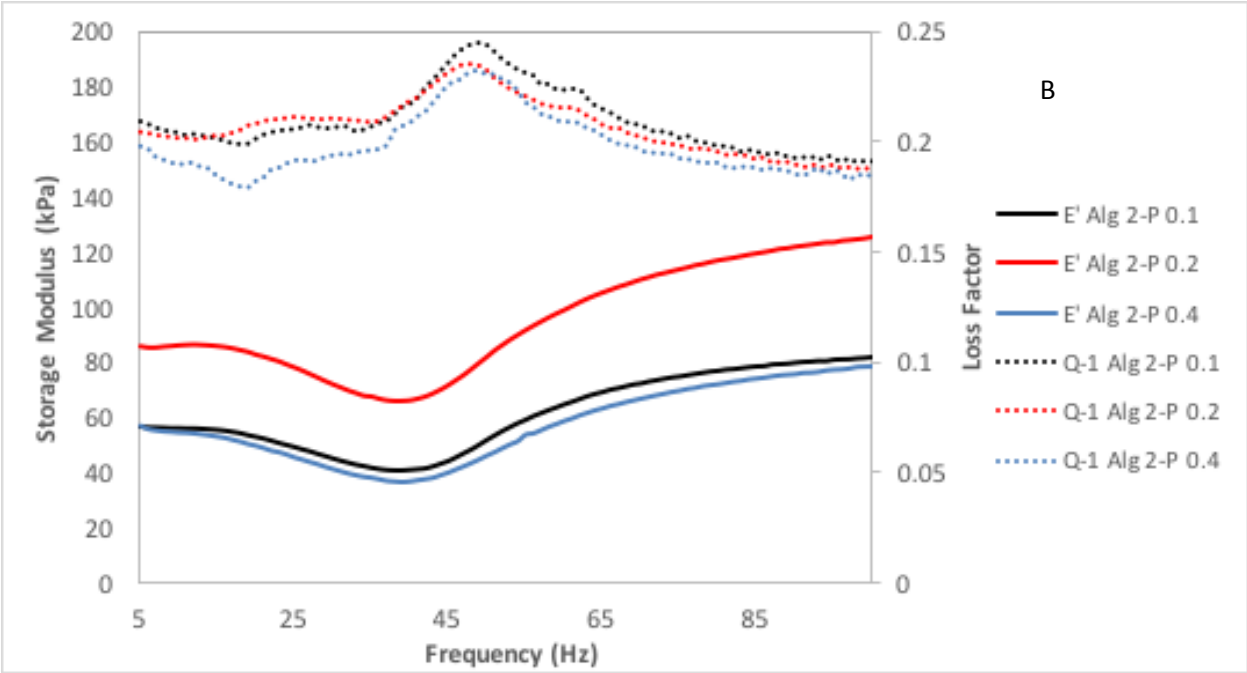
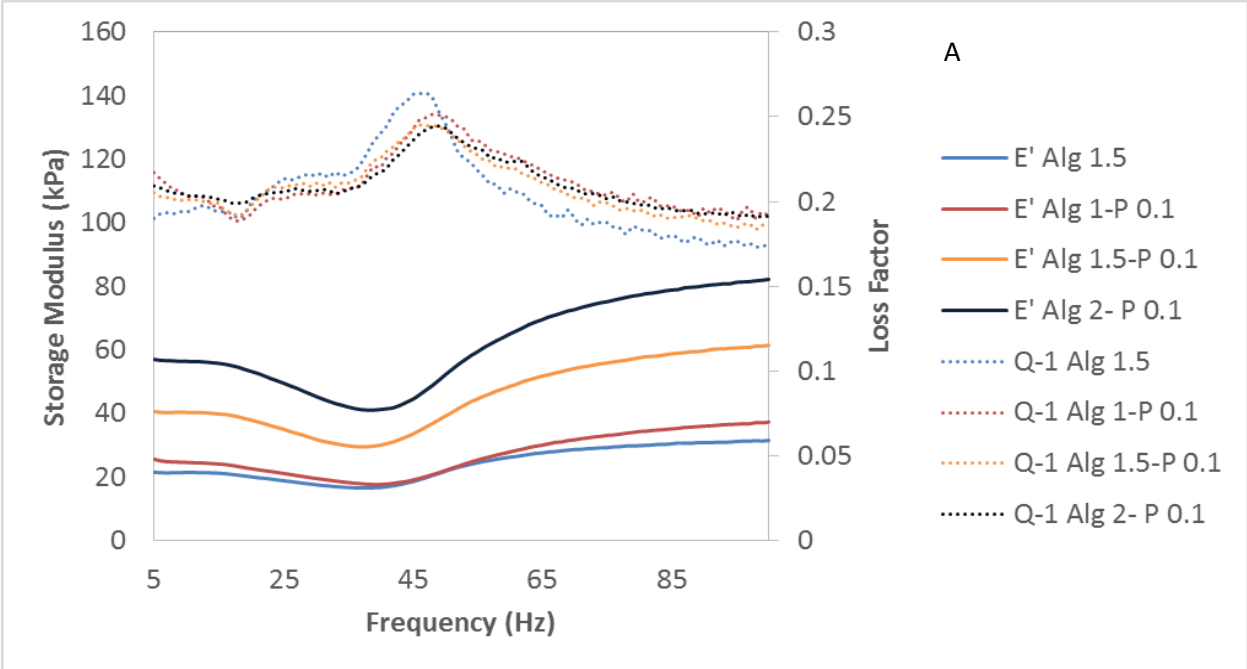


Fig. 5 Storage and loss Factor versus frequency respect to A: alginate variation, B: brushite content variation

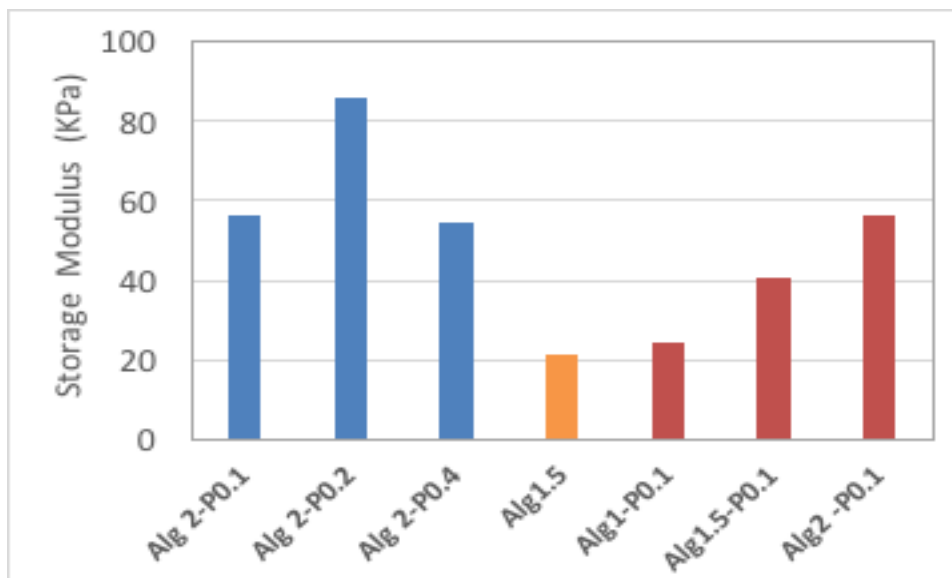


Fig. 6 Effect of the Bru content and Alg concentration on the storage moduli at 10 Hz

3.1.5. Swelling ratio

The release behavior of Alg and of its composites is highly dependent on the swelling ratio and swelling kinetics. In fact, the main release mechanism is based on the swelling behavior. As we can see in the table. 1, the presence of Bru had a good effect on the swelling behavior of the hydrogel so that at the same concentration of Alg the swelling ratio decreased from 12.72 to 10.29. On the other hand, the swelling behaviors of samples were significantly influenced by variation of Alg concentration. The swelling ratio showed an upward trend as the concentration of Alg increased and the content of Bru crystals decreased. We can see that the swelling ratio grew from 7 to 10.29 with a 0.5% increase in the concentration of Alg. This was followed by 1.09 further growth in the sample prepared with 2% of Alg. In addition, the sample Alg 1- P 0.1 had the lowest swelling ratio because in-situ formed Bru crystals restricted the Alg polymer chain movement thus hindering penetration of water into the network. Besides, as the content of

Bru increased in the Alg matrix due to increase in the primary concentration of $(\text{NH}_4)_2\text{HPO}_4$, a slight decrease was detected in swelling ratio of Alg 2-P 0.2 and Alg 2-P 0.4 samples.

Fig.7 shows the swelling kinetics of different samples in PBS media at 37°C . As we can see, the swelling ratio of the samples increased significantly through swelling time passage to reach their maximum ratio. Then, it followed a sharp downward trend with further swelling time passage and even ALg-1.5 and Alg 1- P 0.1 samples experienced disintegration. Osmotic pressure is the main responsible for penetration of water into the polymeric network and consequently weight gain of the samples [37]. Since the strength of $-\text{COO}^- \cdots^+ \text{Ca}^{+2} \cdots^- \text{OOC}$ bonds were at its minimum in the swelling ratio peak, due to the polymer chain expansion, the bonds were easily broken by PO_4^{3-} in the surrounding PBS media. This resulted in disintegration of the Alg, leading to a burst release of the drug.

The significant impact of Bru is considerable in the kinetics of swelling so that the composite samples smoothly gain weight and the disintegration process prolonged further. This can be attributed to Bru crystals resistance against penetration of the PO_4^{3-} functional group and consequently postponed the breakage of $-\text{COO}^- \cdots^+ \text{Ca}^{+2} \cdots^- \text{OOC}$.

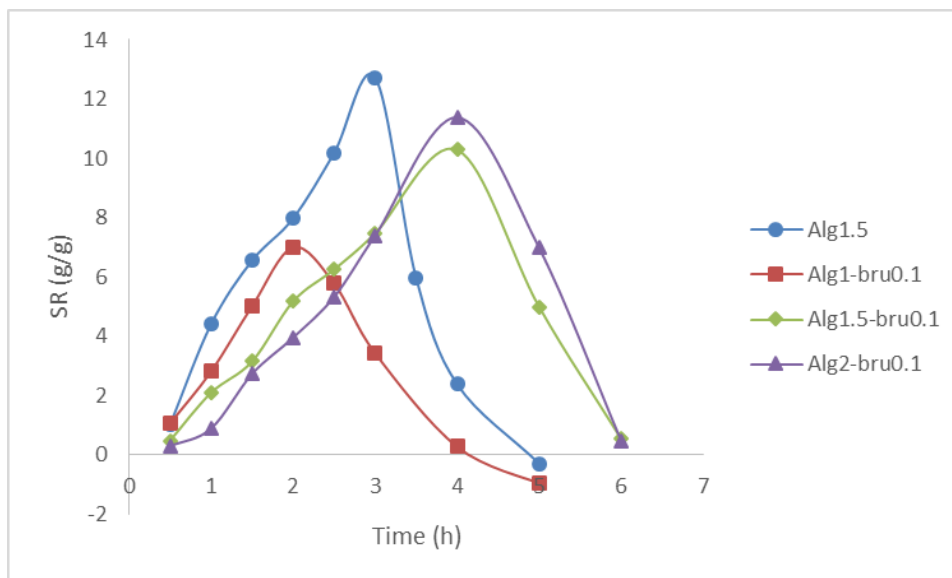


Fig. 7 swelling ratio variation in alginate and alginate-brushite beads in PBS pH 7.4 at different time

3.2. Release behavior

3.2.1 Encapsulation efficiency

The encapsulation efficiencies of the different samples are listed in table. 2. Although we expected that incorporation of Bru into Alg matrix would increase the encapsulation efficiency, due to the formation of a dense surface and retarding the leakage of drug, the results were unexpected. This can be attribute to the fact that presence of Bru has limited the sol-gel transition and made a delay in crosslinking process. Another reason relates to time consuming process of the composite formation and leakage of drug from surface pores. Therefore, more IBU molecules were leaked from the composite samples during fabrication process. Besides, incorporating higher amount of drug resulted in composite beads carrying higher amount of drug. However, what we have to mention is that the significant decreased in EE% does not seem to be ignorable.

Table. 2 preparation conditions and their influence on encapsulation efficiency

Item	Sample	Sodium alginate (wt %)	$[(\text{NH}_4)_2\text{HPO}_4]$ (M)	$\text{Ca}(\text{NO}_3)_2 \cdot 4\text{H}_2\text{O}$ (M)	Ibuprofen (%)	EE (%)
1	Alg 1.5-1	1.5	---	0.2	1	74.97±6.67
2	Alg 1- P 0.1-1	1	0.1	0.2	1	70.02±5.43
3	Alg 1.5- P 0.1-1	1.5	0.1	0.2	1	73.65±16.14
4	Alg 2- P 0.1-1	2	0.1	0.2	1	74.96 ± 2.81
5	Alg 2-P 0.2-1	2	0.2	0.2	1	79.91 ± 2.13
6	Alg 2-P 0.4-1	2	0.4	0.2	1	63.80 ± 2.23
7	Alg 2-P 0.2-1.5	2	0.2	0.2	1.5	67.68 ± 1.15
8	Alg 2-P 0.2-2	2	---	0.2	2	63.24 ± 3.29

3.2.2. Cumulative release

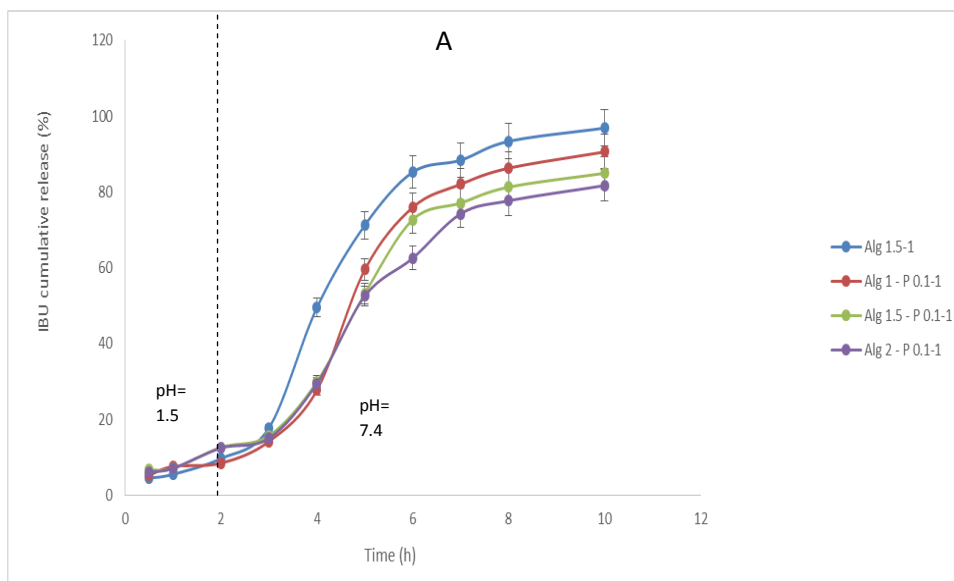
As it is evident in fig. 8, all the formulations demonstrated pH sensitive release behavior. It has been reported that pKa of Alg is almost 3.2 and the transformation of carboxylate group in the Alg chain into -COOH occurs at a pH lower than 3 [38]. Therefore, this transformation established hydrogen bonding between -COOH and hydroxyl group in Alg which restricted the dried beads to swell in simulated gastric fluid. The impact of Alg concentration on cumulative release is illustrated in Fig. 8A. As we can see, the rate of release is not significant owing to low swelling ratio of the samples in acidic condition and all the sample release almost the same level of Ibu. Hence, these results suggest that the IBU was released from the samples by diffusion mechanism. Also, low solubility of IBU in acidic media (simulated gastric fluid) could be another reason for slow release of Ibu from the samples. As discussed before, the formation of Bru within Alg matrix resulted in loading acidic form of Ibu with -COOH carboxyl group into carriers. Therefore, formation of hydrogen bonds between -COOH of Ibu and -COOH of alg is another cause for slow release of Ibu from the carriers in acidic environment. This phenomena was also reported for Diclofenac release from hydrogel based on methacrylated Alg [38]. On the other hand, samples in simulated intestine fluid (pH=7.4) present a total different behavior. All

the samples showed a burst release of IBU owing to extensive swelling in PBS 7.4 and consequently penetration of PO_4^{3-} into the polymer. Besides, all the $-\text{COOH}$ groups in alg and Ibu transformed into $-\text{COO}^-$ at pH 7.4 which not only increased the solubility of Ibu but also, caused electrostatic repulsion between $-\text{COO}^-$ groups and led to faster release of Ibu.

We can see that more than 85% of IBU was released from Ca-Alg samples after 4 hours in PBS 7.4 while, the Alg 2- P 0.1-1 sample release 62% of entrapped IBU at the same time and further 4 hours were need to release 81% of entrapped IBU. Also, we can see that the presence of Bru in the ALG matrix resulted in more than 10% decrease in final IBU release in the Alg 1.5- P 0.1-1 sample. This suggested the positive effect of Alg on release behavior and controlled release of Ibu. Although the sample Alg1- P 0.1-1 had the highest relative content of Bru, the IBU release behavior was almost similar to that of Ca-Alg. This behavior can be explained by the irregular shape of these samples. Unlike the other samples which had the spherical shape, their shape tended to be less spherical due to platelet-like morphology of Bru. In other words, the beads of Alg1-P0.1-1 were less stable than the other composite samples. Hence, the disintegration process accelerated and a higher content of the drug was released.

Next step was evaluating the impact of Bru content on release behavior. Therefore, Alg2-P0.1-1 was chosen as the reference sample because it had the best release profile as well as the beads had a sufficient stability so that the beads would remain stable following the increase in the content of $(\text{NH}_4)_2\text{HPO}_4$. As plotted in Fig. 8.B the cumulative release decreased when the primary concentration of $(\text{NH}_4)_2\text{HPO}_4$ was 0.2 M. The Bru crystals resisted against swelling and following PO_4^{3-} penetration. Further increase in the concentration of $(\text{NH}_4)_2\text{HPO}_4$ had a negative impact on the release profile since the beads were less crosslinked than the other two samples and disable to restrict release of IBU. Furthermore, Fig. 8C demonstrates how initial drug

content would change the release profile. It is clear that the Alg 2- P 0.2-1.5 sample follows almost the same pattern of release as Alg 2- P 0.2-1 sample when the incorporated drug increased up to 0.5%. Further increase in the content of drug possibly had reverse effect on the release profile owing to intermolecular crosslinking between sodium IBU and sodium Alg, sodium IBU and Bru. As a result, less stable beads were formed in a way that the beads exhibit less resistance against penetration of Ibu to the surrounding media. Hence, these results indicate that an increasing in the drug content not only decreased the EE%, but also it had a reverse effect on release profile.



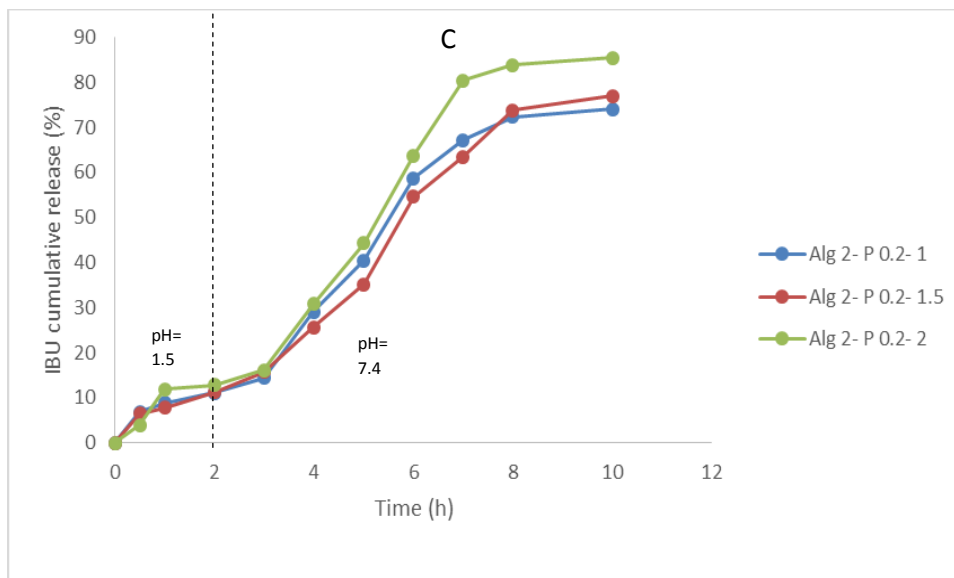
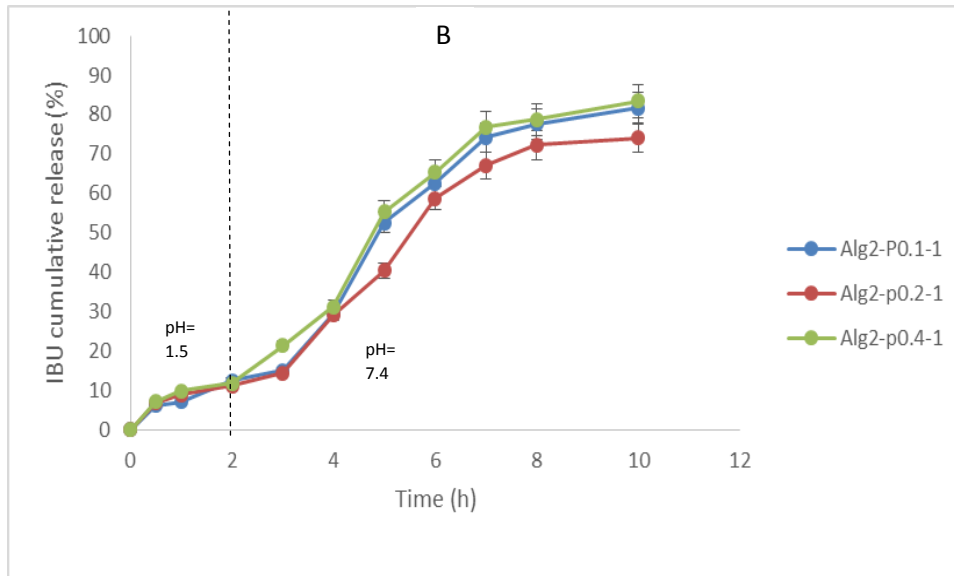


Fig. 8 cumulative release versus time in pH 1.5 followed by pH 7.4 A: alginate variation, B: brushite content variation, C: drug content variation

Conclusion

The current study was carried out to evaluate in-situ synthesized Alg-Bru as a new potential reinforced carrier for delivering drug and other active biomolecules. IBU was actively loaded in the carriers during crosslinking and formation of Bru within Alg matrices. According to FT-IR and XRD results the composite materials were successfully fabricated and the drug was loaded into the carriers. SEM images demonstrated the significant impact of Bru crystals on the morphology of the beads.

The restriction of Alg chain movement by uniformly dispersed Bru crystals was the main cause for regulating swelling behavior and enhancing the mechanical behavior. Furthermore, improving the swelling behavior consequently caused the gradual release in composite samples and avoided burst release which was experienced in the case of calcium Alg beads and the optimal formulation prolonged IBU release for a period of 10 hours. These results allow us to suggest that the in-situ synthesis of Bru within Alg sufficiently modified release behavior. However, the entrapment efficiency was not remarkably improved in comparison with that of calcium Alg. Simplicity along with effectiveness of the used method in the present study to fabricate a carrier with gradual release behavior can be further improved to encapsulate bioactive molecules including other drugs, proteins, vitamins for a prolonged release as well as reduced the risk of high dosage.

References

1. Rangasamy, Manivannan, and Kugalur Ganesan Parthiban. "Recent advances in novel drug delivery systems." *IJRAP* 1.2 (2010): 316-26.
2. Wu, Jie, et al. "A thermosensitive hydrogel based on quaternized chitosan and poly (ethylene glycol) for nasal drug delivery system." *Biomaterials* 28.13 (2007): 2220-2232.
3. Jabeen, Suraya, et al. "Rheological behavior and Ibuprofen delivery applications of pH responsive composite alginate hydrogels." *Colloids and Surfaces B: Biointerfaces* 139 (2016): 211-218.

4. Zhao, Pengkun, et al. "A study of chitosan hydrogel with embedded mesoporous silica nanoparticles loaded by ibuprofen as a dual stimuli-responsive drug release system for surface coating of titanium implants." *Colloids and Surfaces B: Biointerfaces* 123 (2014): 657-663.
5. Oun, Rabbab, Jane A. Plumb, and Nial J. Wheate. "A cisplatin slow-release hydrogel drug delivery system based on a formulation of the macrocycle cucurbit [7] uril, gelatin and polyvinyl alcohol." *Journal of inorganic biochemistry* 134 (2014): 100-105.
6. de Figueiredo, Ingrid Samantha Tavares, et al. "Efficacy of a membrane composed of polyvinyl alcohol as a vehicle for releasing of wound healing proteins belonging to latex of *Calotropis procera*." *Process Biochemistry* 49.3 (2014): 512-519.
7. Loh, Xian Jun, et al. "Controlled drug release from biodegradable thermoresponsive physical hydrogel nanofibers." *Journal of Controlled Release* 143.2 (2010): 175-182.
8. González-Rodríguez, M. L., et al. "Alginate/chitosan particulate systems for sodium diclofenac release." *International Journal of Pharmaceutics* 232.1 (2002): 225-234.
9. Pawar, Siddhesh N., and Kevin J. Edgar. "Alginate derivatization: a review of chemistry, properties and applications." *Biomaterials* 33.11 (2012): 3279-3305.
10. Lee, Kuen Yong, and David J. Mooney. "Alginate: properties and biomedical applications." *Progress in polymer science* 37.1 (2012): 106-126.
11. Phillips, Glyn O., and Peter A. Williams, eds. *Handbook of hydrocolloids*. Elsevier, 2009.
12. Goh, Cheong Hian, Paul Wan Sia Heng, and Lai Wah Chan. "Alginates as a useful natural polymer for microencapsulation and therapeutic applications." *Carbohydrate Polymers* 88.1 (2012): 1-12.
13. Lee, Sungmun, Yeu-Chun Kim, and Ji-Ho Park. "Zein-alginate based oral drug delivery systems: Protection and release of therapeutic proteins." *International Journal of Pharmaceutics* 515.1 (2016): 300-306.
14. Boonthekul, Tanyarut, Hyun-Joon Kong, and David J. Mooney. "Controlling alginate gel degradation utilizing partial oxidation and bimodal molecular weight distribution." *Biomaterials* 26.15 (2005): 2455-2465.
15. Maiti, Sabyasachi, et al. "Adipic acid dihydrazide treated partially oxidized alginate beads for sustained oral delivery of flurbiprofen." *Pharmaceutical development and technology* 14.5 (2009): 461-470.
16. Wang, Qin, Junping Zhang, and Aiqin Wang. "Preparation and characterization of a novel pH-sensitive chitosan-g-poly (acrylic acid)/attapulgitite/sodium alginate composite hydrogel bead for controlled release of diclofenac sodium." *Carbohydrate Polymers* 78.4 (2009): 731-737.
17. Wang, Qin, et al. "Preparation and swelling properties of pH-sensitive composite hydrogel beads based on chitosan-g-poly (acrylic acid)/vermiculite and sodium alginate for diclofenac controlled release." *International journal of biological macromolecules* 46.3 (2010): 356-362.
18. Viseras, C., et al. "Biopolymer-clay nanocomposites for controlled drug delivery." *Materials Science and Technology* 24.9 (2008): 1020-1026.
19. Kim, H- J., et al. "Ultrasound- Triggered Smart Drug Release from a Poly (dimethylsiloxane)-Mesoporous Silica Composite." *Advanced Materials* 18.23 (2006): 3083-3088.
20. Wang, Shao-Feng, et al. "Preparation and mechanical properties of chitosan/carbon nanotubes composites." *Biomacromolecules* 6.6 (2005): 3067-3072.
21. Zhang, Xiaolan, et al. "Alginate microsphere filled with carbon nanotube as drug carrier." *International journal of biological macromolecules* 47.3 (2010): 389-395.

22. Zhang, Junping, Qin Wang, and Aiqin Wang. "In situ generation of sodium alginate/hydroxyapatite nanocomposite beads as drug-controlled release matrices." *Acta Biomaterialia* 6.2 (2010): 445-454.
23. Ilie, Andreia, et al. "New composite materials based on alginate and hydroxyapatite as potential carriers for ascorbic acid." *International journal of pharmaceutics* 510.2 (2016): 501-507.
24. Hasnain, M. Saquib, et al. "Alginate-based bipolymeric-nanobioceramic composite matrices for sustained drug release." *International journal of biological macromolecules* 83 (2016): 71-77.
25. Tamimi, Faleh, Zeeshan Sheikh, and Jake Barralet. "Dicalcium phosphate cements: Brushite and monetite." *Acta biomaterialia* 8.2 (2012): 474-487.
26. Dabiri, Seyed Mohammad Hossein, et al. "Characterization of alginate-brushite in-situ hydrogel composites." *Materials Science and Engineering: C* 67 (2016): 502-510.
27. Dabiri, Seyed Mohammad Hossein, et al. "Letter to editor for supporting "Characterization of alginate-brushite in-situ hydrogel composites". " *Materials Science and Engineering: C* 74 (2017): 410-412.
28. Hirsch, Anna, et al. "Infrared Absorption Spectrum of Brushite from First Principles." *Chemistry of Materials* 26.9 (2014): 2934-2942.
29. Štulajterová, R., and L. Medvecký. "Effect of calcium ions on transformation brushite to hydroxyapatite in aqueous solutions." *Colloids and Surfaces A: Physicochemical and Engineering Aspects* 316.1 (2008): 104-109.
30. Amer, Walid, et al. "Smart designing of new hybrid materials based on brushite-alginate and monetite-alginate microspheres: Bio-inspired for sequential nucleation and growth." *Materials Science and Engineering: C* 35 (2014): 341-346.
31. Ribeiro, C. C., C. C. Barrias, and M. A. Barbosa. "Calcium phosphate-alginate microspheres as enzyme delivery matrices." *Biomaterials* 25.18 (2004): 4363-4373.
32. Jubert, Alicia, et al. "Vibrational and theoretical studies of non-steroidal anti-inflammatory drugs Ibuprofen [2-(4-isobutylphenyl) propionic acid]; Naproxen [6-methoxy- α -methyl-2-naphthalene acetic acid] and Tolmetin acids [1-methyl-5-(4-methylbenzoyl)-1H-pyrrole-2-acetic acid]." *Journal of molecular structure* 783.1 (2006): 34-51.
33. Horcajada, Patricia, et al. "Controlled release of Ibuprofen from dealuminated faujasites." *Solid State Sciences* 8.12 (2006): 1459-1465.
34. Bjørnøy, Sindre H., et al. "Letter to the Editor re" Characterization of alginate-brushite in-situ hydrogel composites." *Materials science & engineering. C, Materials for biological applications* 70.Pt 1 (2017): 930.
35. Angadi, Sudha C., Lata S. Manjeshwar, and Tejraj M. Aminabhavi. "Novel composite blend microbeads of sodium alginate coated with chitosan for controlled release of amoxicillin." *International journal of biological macromolecules* 51.1 (2012): 45-55.
36. Marrella, A., et al. "Enhanced mechanical performances and bioactivity of cell laden-graphene oxide/alginate hydrogels open new scenario for articular tissue engineering applications." *Carbon* 115 (2017): 608-616.
37. Lee, Wen- Fu, and Ren- Jey Wu. "Superabsorbent polymeric materials. II. Swelling behavior of crosslinked poly [sodium acrylate- co- 3- dimethyl (methacryloyloxyethyl) ammonium propane sulfonate] in aqueous salt solution." *Journal of applied polymer science* 64.9 (1997): 1701-1712.
38. Zhao, Jun, et al. "Multifunctional interpenetrating polymer network hydrogels based on methacrylated alginate for the delivery of small molecule drugs and sustained release of protein." *Biomacromolecules* 15.9 (2014): 3246-3252.

Supporting information for:

New in-situ synthesized hydrogel composite based on alginate and brushite as a potential pH sensitive drug delivery system

Seyed Mohammad Hossein Dabiri*, Alberto Lagazzo, Fabrizio Barberis, Amirreza Shayganpour, Elisabetta Finocchio, Laura Pastorino

Submitted to Carbohydrate Polymers journal

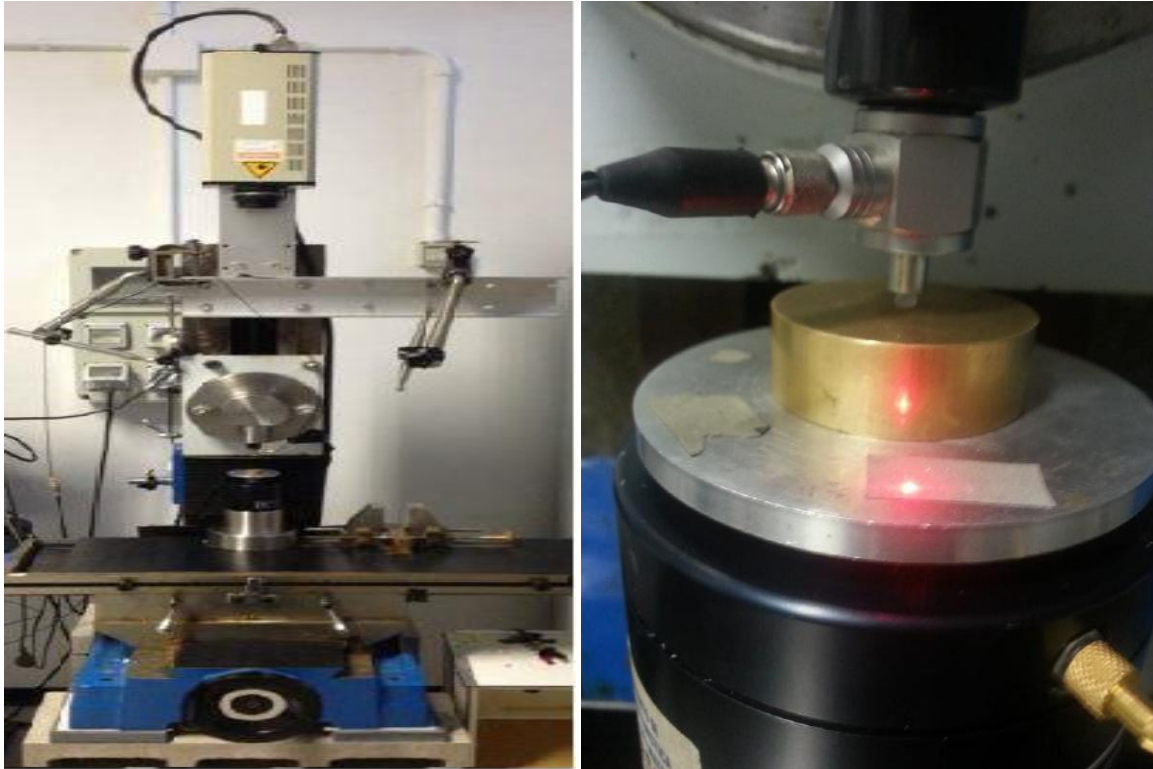


Fig.S1 schematic of the DMA test equipment to obtain storage and loss modulus

The experimental set-up poses following items:

- Fixed head movable by a screw, so that the distance between the two plates can be adjusted accordingly with the sample dimensions.
- Electrodynamic mini-shaker (Brüel & Kjær type 4810): it is provided with a permanent field magnet and it applies oscillating stimuli to the implant.
- Power amplifier (Brüel & Kjær type 2706): it controls the mini-shaker and the amplification magnitude of the sinusoidal vibrations can be set through a potentiometer.
- Force transducer: it consists of a piezoelectric load cell, which generates a charge signal (proportional to the applied force) as a response to the mechanical stimulus applied by the shaker.
- Laser vibrometer (Complete Polytec Laser Vibrometer System OFV 3000/302 with Nikon Lens Sensor Head Version): it's located above the experimental set-up and it

measures the displacement. This component works on the principle of optical interference: a laser

- beam is aimed towards a target plate, leading to light scattering. The light that has been scattered is then collected and it interferes with a reference beam.
- Metal plate placed over the mini-shaker and used as a reflecting surface for the laser beam.
- Sensor signal conditioning (482C series, PCB Piezotronics): it amplifies and converts the signal acquired by the force transducer into an electrical one.
- Labview software responsible for the functioning of the instrument, and for storing, displaying and processing measurement data. The instrument is isolated from vibration by blocks of cement and rubber supports.

Table. S1 set up parameter for the DMA tests

Initial deformation	20% of initial diameter
Amplitude	5.00 V
Start frequency	5.00 Hz
Stop frequency	100.00 Hz
Stimulus	9.73 N/V